Phytomedicine 76 (2020) 153251

Contents lists available at ScienceDirect

Phytomedicine

journal homepage: www.elsevier.com/locate/phymed

The combination of *Panax ginseng* and *Angelica sinensis* alleviates ischemia brain injury by suppressing NLRP3 inflammasome activation and microglial pyroptosis

Jia Hu[a,1], Cheng Zeng[a,1], Jie Wei[b], Fengqi Duan[a], Sijun Liu[a], Yonghua Zhao[c,**], Hongmei Tan[a,*]

[a] Department of Pathophysiology, Zhongshan School of Medicine, Sun Yat-sen University, Guangzhou 510080, China
[b] Department of Pharmacology, Guangxi Institute of Chinese Medicine and Pharmaceutical Science, Nanning, Guangxi 530022, China
[c] State Key Laboratory of Quality Research in Chinese Medicine, Institute of Chinese Medical Sciences, University of Macau, Macao SAR, China

ARTICLE INFO

Keywords:
Ischemic stroke
CPA
NLRP3 inflammasomes
Pyroptosis

ABSTRACT

Background: The combination of *Panax ginseng* and *Angelica sinensis* (CPA) has been used to treat stroke for one thousand years and demonstrated clinically to have satisfied effects. However, the underlying mechanism remains unknown.

Purpose: We investigate whether CPA has neuroprotective effects via suppressing Nod-like receptor protein 3 (NLRP3) inflammasome and microglial pyroptosis against ischemic injury in transient middle cerebral artery occlusion (MCAO) rats.

Methods: Male rats were divided randomly into sham operated, MCAO, MCC950 (NLRP3-specific inhibitor) and CPA groups. Neurological deficits, glucose uptake, infarct size, activation of NLRP3 inflammasomes, microglial pyroptosis and related signaling pathways were detected. BV-2 microglial cells subjected to oxygen-glucose deprivation/reoxygenation (OGD/R) were used in *in vitro* experiments.

Results: Compared with sham rats, elevated level of proinflammatory interleukin-1β (IL-1β) in plasma, neurological function deficit, reduced glucose uptake in ipsilateral hemisphere, obvious infarct size, the activation of NLRP3 inflammasomes and enhanced microglial pyroptosis were presented in MCAO rats. The administrations of MCC950 and CPA respectively reversed the results. In vitro OGD/R induced the release of lactate dehydrogenase, promoted NLRP3 inflammasomes activation and pyroptosis in BV-2 cells, which was significantly suppressed by treatment with ginsenoside Rd (Rd) and Z-ligustilide (LIG). Mechanistically, OGD/R induced high expression of dynamin-related protein 1 (Drp1) and mitochondrial fission, as well as NLRP3 inflammasomes activation and pyroptosis in BV-2 cells, which was attenuated by treatment with Rd and LIG. Moreover, the increased expression of Drp1 was validated in MCAO rats, and also abolished by MCC950 or CPA treatments.

Conclusion: CPA treatment attenuates cerebral injury via inhibition of NLRP3 inflammasomes activation and microglial pyroptosis after stroke, which at least partially involved in the amelioration of Drp1-mediated mitochondrial fission.

Introduction

Ischemic stroke is one of the most common cerebrovascular diseases, which causes severe and long-term disability, and even death. The mechanisms underlying stroke-induced injury are complicated. Previous report demonstrated that inflammatory response played an important role in the

Abbreviations: ASC, apoptosis-associated speck-like protein containing a CARD; CPA, the combination of *Panax ginseng* and *Angelica sinensis*; Drp1, dynamin-related protein 1; GSDMD, gasdermin D; GSDMD-NT, N-terminal fragment of gasdermin D; IL-1β, interleukin-1β; MCAO, middle cerebral artery occlusion; NLRP3, Nod-like receptor protein 3; OGD/R, oxygen-glucose deprivation/reoxygenation; ROI, regions of interest; SUV, standardized uptake value; TLR, toll-like receptor; TTC, 2,3,5-triphenyl four azole nitrogen chloride; TUNEL, TdT-mediated dUTP nick end labeling; LIG, Z-ligustilide

* Corresponding authors. Department of Pathophysiology, Zhongshan School of Medicine, Sun Yat-sen University, #74, Zhongshan Road 2, Guangzhou, Guangdong, China 510080, Tel: (8620) 87334055; fax: (8620) 87330026

** Co-corresponding authors. Research Building N22, Institute of Chinese Medical Sciences, University of Macau, Avenida da Universidade, Taipa, Macau, 999078, China. Tel: (853) 88224877, Fax: (853) 28841358

E-mail addresses: yonghuazhao@um.edu.mo (Y. Zhao), tanhm@mail.sysu.edu.cn (H. Tan).

[1] These authors contributed equally to this work.

https://doi.org/10.1016/j.phymed.2020.153251
Received 27 February 2020; Received in revised form 2 May 2020; Accepted 23 May 2020

pathogenesis of ischemic stroke (Lambertsen et al., 2012). Pro-inflammatory cytokines such as interleukin-1β (IL-1β) are increased in the brain tissue of middle cerebral artery occlusion (MCAO) rats. However, the detailed mechanism of inflammatory modulation after ischemic stroke remains largely elusive.

The inflammasome has critical influence on the initiation and the progression of innate immune responses in the central nervous system (Schroder and Tschopp, 2010). The Nod-like receptor protein 3 (NLRP3) inflammasome consists of NLRP3, the adaptor protein apoptosis-associated speck-like protein containing a caspase recruitment domain (ASC) and inflammatory caspase-1. The signaling of NLRP3 inflammasomes is an essential mechanism in mediating inflammatory response in the process of cardiovascular disorder, diabetes and ischemic stroke (Fann et al., 2013). Recent study highlighted that NLRP3 inflammasome deficiency or its selective inhibitor ameliorated cerebral injury after ischemic stroke (Ismael et al., 2018). NLRP3 inflammasome activation generally includes two processes: a priming event that induces NF-κB signaling transduction, leading to the increased expression of NLRP3, precursors of caspase-1 (pro-caspase-1) and IL-1β (pro-IL-1β) via toll-like receptor (TLR)/NF-κB signaling, and the subsequent assembly of NLRP3 with ASC and pro-caspase-1. NLRP3 inflammasome assembly triggers the activation of inflammatory caspase-1 and process of pro-inflammatory cytokines such as pro-IL-1β (Davis et al., 2011). In addition, caspase-1 is recognized to mediate a novel form of programmed cell death termed as pyroptosis. The hallmark characteristics of pyroptosis are pore formation, osmotic swelling and early loss of membrane integrity. The active caspase-1 cleaves gasdermin D (GSDMD) to generate an N-terminal GSDMD fragment (GSDMD-NT), which was identified as a critical executor of pyroptosis by inducing the formation of membrane pores (Zeng et al., 2019). It was reported that active caspase-1 led to pyroptosis in microglia through intramembranous pores (Barrington et al., 2017). Therefore, targeting the NLRP3 inflammasome and pyroptosis to suppress the excessive inflammatory response may develop a novel therapeutic strategy for cerebral ischemia.

As common traditional Chinese herbal medicines, the combination of *Panax ginseng* and *Angelica sinensis* (CPA) are used to treat stroke for one thousand years and demonstrated clinically to have satisfied efficacies on various neurological disorders (Luo et al., 2019). As representative compound of *Panax ginseng*, ginsenoside Rd exhibits prominent effect on suppressing oxidative stress and inflammation in cerebral ischemic rats, colitis and Alzheimer's disease (Hu et al., 2013; Ye et al., 2011). *Angelica sinensis* and its active ingredients reduced the size of cerebral infarction and improved neurological deficits by minimizing oxidative stress and anti-apoptosis in MCAO rats (Kuang et al., 2006). Its ingredients, volatile oils and Z-ligustilide (LIG), exerted anti-inflammatory effect in atherosclerotic apoE$^{-/-}$ mice and acute inflammation rat model (Li et al., 2016). However, whether CPA and its active ingredients have the efficacy on suppressing NLRP3 inflammasomes activation and microglial pyroptosis remains unknown. In the current study, the extract derived from the two kinds of herbal medicine is used for treating transient MCAO model in rats, and the representative ingredients ginsenoside Rd and LIG are employed for oxygen-glucose deprivation/reoxygenation (OGD/R)-induced BV2 microglial cells. We investigate the neuroprotective effect and discover the related mechanisms.

Materials and methods

Materials

Detailed drugs and reagents are provided in the attached supplemental material.

The establishment of animal ischemic stroke model and groups division

Male Sprague–Dawley (SD) rats (250 - 300 g) were obtained from Medical Laboratory Animal Center of Guangdong Province. All animals were kept in certified specific pathogen-free facilities maintained around 24 ℃ with a 12 h light/dark cycle and free access to food and water. The animal experiment was approved by the Animal Care Committee of Sun Yat-sen University and was performed in accordance with NIH Guide for the Care and Use of Laboratory Animals. To select appropriate dose of CPA to conduct the following analysis, rats were randomly divided into four groups: Sham-operated group, MCAO group, low dosage of CPA (L-CPA) group, and high dosage of CPA (H-CPA) group. 4.5 g/kg and 9 g/kg of CPA were administered intragastrically to rats in L-CPA and H-CPA groups with once daily for 3 days prior to MCAO operation and for 7 days after MCAO, respectively. The rats were assessed for neurological deficit score and cerebral infarction via 2, 3, 5-triphenyltetrazolium chloride (TTC) staining.

According to the above experimental results, the appropriate dose of CPA was selected for the following experiment. Rats were randomized divided into four groups: sham-operated group, MCAO group, CPA group and MCC950 group (n = 10 ~ 12 for each group). Animals in MCAO, CPA and MCC950 groups were subjected to MCAO for 2 h followed by reperfusion using the intraluminal suture model. Rats in MCC950 group were intraperitoneal injected with 5 mg/kg/d of MCC950 for 7 consecutive days after MCAO. At day 7 after operation, all rats were sacrificed, and their blood samples were collected and brain tissue was harvested immediately.

Neurological function assessment

Detailed method was described in supplementary material.

^{18}F -FDG- micro-PET /CT images and analysis

The glucose metabolism measured by^{18}F-2-deoxy-glucose (FDG)-PET /CT imaging was performed according to the protocol described in previous report (Wang et al., 2013). Regions of interests (ROIs) 2 mm in diameter were drawn on the ipsilateral and contralateral hemispheres to measure the amount of glucose metabolism in different parts of the brain. The relative metabolic activity, standardized uptake value (SUV), was measured in the ROI. The lesion-to-normal homologous contralateral (L/N) ratio was calculated with the following formula: metabolic SUV of lesion site ROI/metabolic SUV of contralateral site ROI.

Infarct size assessment

At the end of the experiment, the brain was harvested and kept at −20 ℃ for 40 min. Then the frozen brains were sliced into uniform coronal sections of approximately 2 mm thickness which were stained with TTC. The unstained (white) area indicates infracted tissue and the stained (red) area indicates normal tissue. To correct for brain swelling, the infarct area was determined by indirect method according to the following formula: right infarct area = left hemisphere area − non-infarcted area in the right hemisphere. Then the total infarct area for all slices of each brain was integrated and percentage of ipsilateral infarct area was calculated (n = 5 ~ 6 for each group) (Fann et al., 2013).

ELISA assay for Plasma IL-1β and Immunofluorescent staining

Detailed method was described in supplementary material.

Oxygen-glucose deprivation/reoxygenation

BV-2 microglial cells were obtained from China Center for Type Culture Collection (Wuhan, China). Cells were incubated with Rd (0.1, 1.0, 10 μmol/l) and LIG (1, 2.5, 10 μmol/l) alone or in combination at different concentrations for 2 h, and then exposed to OGD/R. Briefly, the cells were cultured in DMEM medium without glucose and placed inside a chamber for 3 hours with a premixed gas (0.2% O_2, 94.8% N2,

5% CO_2). Then BV-2 cells returned to normal culture condition for 24 hours. Cells incubated with a selective NLRP3 inhibitor MCC950 (10 μmol/l) was served as the positive control.

Cell viability, lactate dehydrogenase and Mitochondrial morphology assays

Detailed method was described in supplementary material.

Analysis of pyroptotic cell

Brain sections were triple immunofluorescent stained with anti-active caspase-1 antibody, TdT-mediated dUTP nick end labeling (TUNEL) and anti-Iba-1 antibody (active microglia marker). Cell slides were double immunofluorescent stained with TUNEL and anti-active caspase-1 antibody. The slides were subjected to examinations using a confocal laser scanning microscope (LSM780, Zeiss, Germany). Active caspase-1^+/TUNEL$^+$ cells were designated as pyroptotic cells.

Drp1 plasmid transfection

Cells were transfected with the pcDNA-encoding Drp1 protein plasmid or the mock GV362 vector using Lipofectamine 3000 following the manufacturer's instructions. After 48 hours transfection, cells were washed and incubated with Rd and LIG alone or in combination for 2 hours, and then exposed to OGD/R. Cells were harvested for western blot or immunofluorescent staining.

Western blot

Western blot procedures were carried out using standard protocol with specific antibodies against NLRP3, caspase-1, IL-1β, Drp1 and GSDMD. The blots were visualized using a ChemiDoc™ Touch Imaging System (Bio Rad, CA, USA). Quantification of band intensity was carried out using Image J software (NIH, Bethesda, MD, USA).

Statistical analysis

Data are shown as the mean ± SD. Statistical comparison among multiple groups was carried out by one-way ANOVA followed by LSD test. The non-parametric Kruskal– Wallis test and Dunn's Multiple Comparison test were used for the nonparametric comparison of neurological deficit scores. Differences were considered significant for $p < 0.05$.

Results

Dose selection of CPA for further MCAO experiment

We investigated neuroprotective efficacy of CPA at different doses in MCAO rats. Rats in MCAO group exhibited neurological deficit and obvious cerebral infarction, which were reversed by high dose of CPA administration (Fig. 1A-C). Based on these data, high dose of CPA was considered for further studies.

CPA treatment attenuated cerebral injury

Rats in MCAO group obviously presented neurological deficit after 48 h reperfusion, which was improved by the administration of CPA or MCC950 (Fig. 2A). At day 7 after reperfusion, glucose uptake in ipsilateral hemisphere significantly decreased in MCAO rats, which was increased by the administration of CPA or MCC950 (Fig. 2B-C). CPA or MCC950 treatment also attenuated MCAO-induced cerebral infarction at day 7 after reperfusion (Fig. 2D-E). Collectively, these results indicated that treatment with CPA or MCC950 significantly decreased MCAO-induced cerebral damage and improved neurological function.

CPA treatment suppressed MCAO-induced NLRP3 inflammasome activation

MCAO induced NLRP3 inflammasomes activation in the ischemic region as evidenced by increased expression of NLRP3, cleavage of caspase-1 and IL-1β and colocalization of NLRP3 inflammasome components (NLRP3 and caspase-1). Importantly, MCAO-induced NLRP3 inflammasomes activation was inhibited by the administration of CPA (Fig. 3A-C). Consistent with NLRP3 inflammasomes activation, plasma IL-1β also significantly increased in MCAO rats, which was suppressed by the treatment of CPA (Fig. 3D). The inhibitory effect of CPA on NLRP3 inflammasomes activation was comparable to that of MCC950.

CPA treatment reduced MCAO-induced microglial pyroptosis

Our data showed that MCAO significantly induced the expression and cleavage of GSDMD in ischemic region (Fig. 4A-B), indicating the

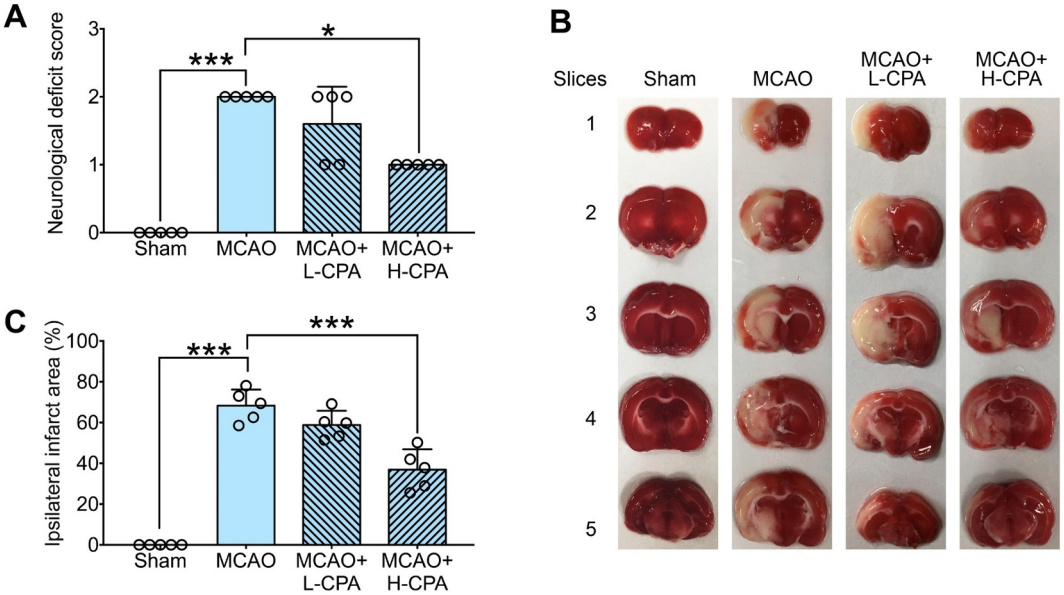

Fig. 1. Dose selection of CPA. (**A**) Neurological deficit scores 48 hours post-MCAO, n = 5. (**B**) Representative images of TTC staining and (**C**) ipsilateral infarct area at day 7 after MCAO, n = 5. * $p < 0.05$, *** $p < 0.001$.

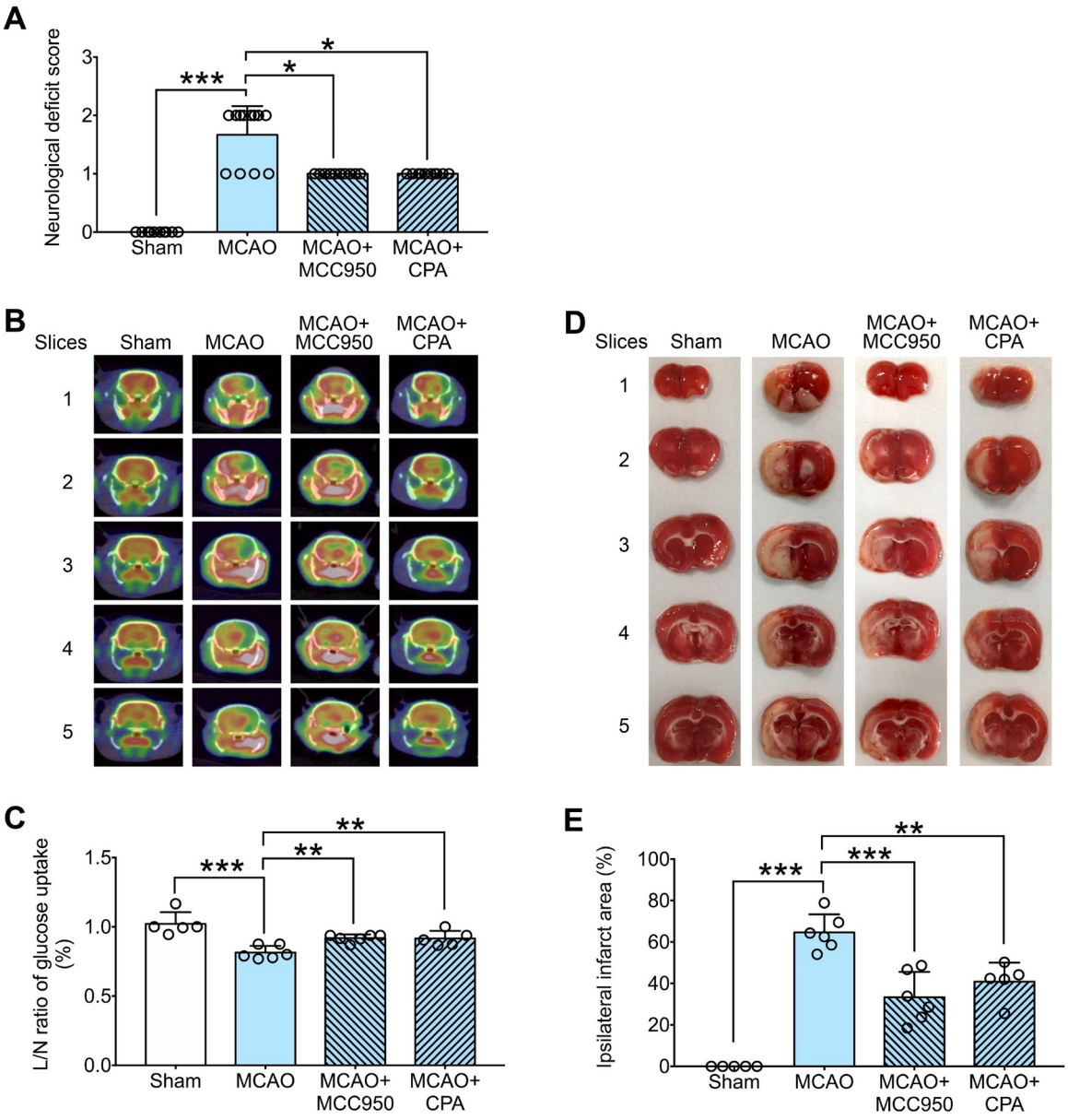

Fig. 2. CPA treatment decreased cerebral damage in MCAO rats. (**A**) Neurological deficit scores 48 hours post-MCAO, n = 10 ~ 12. (**B**) Representative ^{18}F-FDG PET/CT images and (**C**) L/N ratio of glucose uptake value at day 7 after MCAO, n = 5 ~ 6. (**D**) Representative images of TTC staining and (**E**) ipsilateral infarct area at day 7 after MCAO, n = 5 ~ 6. * $p < 0.05$, ** $p < 0.01$, *** $p < 0.001$.

presence of pyroptosis in MCAO rats. Further study showed that no pyroptotic cell was detected in the brain tissue of sham rats. In contrast, pyroptosis was obviously observed in ischemic region of MCAO rats. Interestingly, the majority of pyroptotic cells was microglia (Fig. 4C-D). Importantly, treatment with CPA or MCC950 inhibited MCAO-induced cleavage of GSDMD and reduced the number of pyroptotic microglia (Fig. 4A-D). These results suggested that MCAO-induced microglial pyroptosis was suppressed by treatment with CPA or MCC950.

Ginsenoside Rd and Z-Ligustilide decreased OGD/R-induced BV-2 cell injury

Compared to controls, OGD/R significantly impaired cell viability, which was reversed by treatment with Rd at 1.0 and 10 μmol/l and LIG at 2.5 and 10 μmol/l. Based on these data, 1.0 μmol/l of Rd and 2.5 μmol/l of LIG was applied to further investigate in the following experiments (Fig. 5A-B). Further results showed that treatment with Rd and LIG alone or in combination, or MCC950 ameliorated OGD/R-induced microglial cell injury, as evidenced by improved cell viability and decreased LDH release (Fig. 5C-D).

Ginsenoside Rd and Z-Ligustilide suppressed OGD/R-induced NLRP3 inflammasomes activation and pyroptosis in BV-2 cells

Our data showed that OGD/R significantly increased the expression of NLRP3, the cleavage of caspase-1, IL-1β and GSDMD in BV-2 cells (Fig. 6A-D), indicating OGD/R-induced NLRP3 inflammasomes activation and pyroptosis in BV-2 cells. Results also showed that OGD/R induced about 27.2% of pyroptotic cells (Caspase-1$^+$/TUNEL$^+$ cells) in

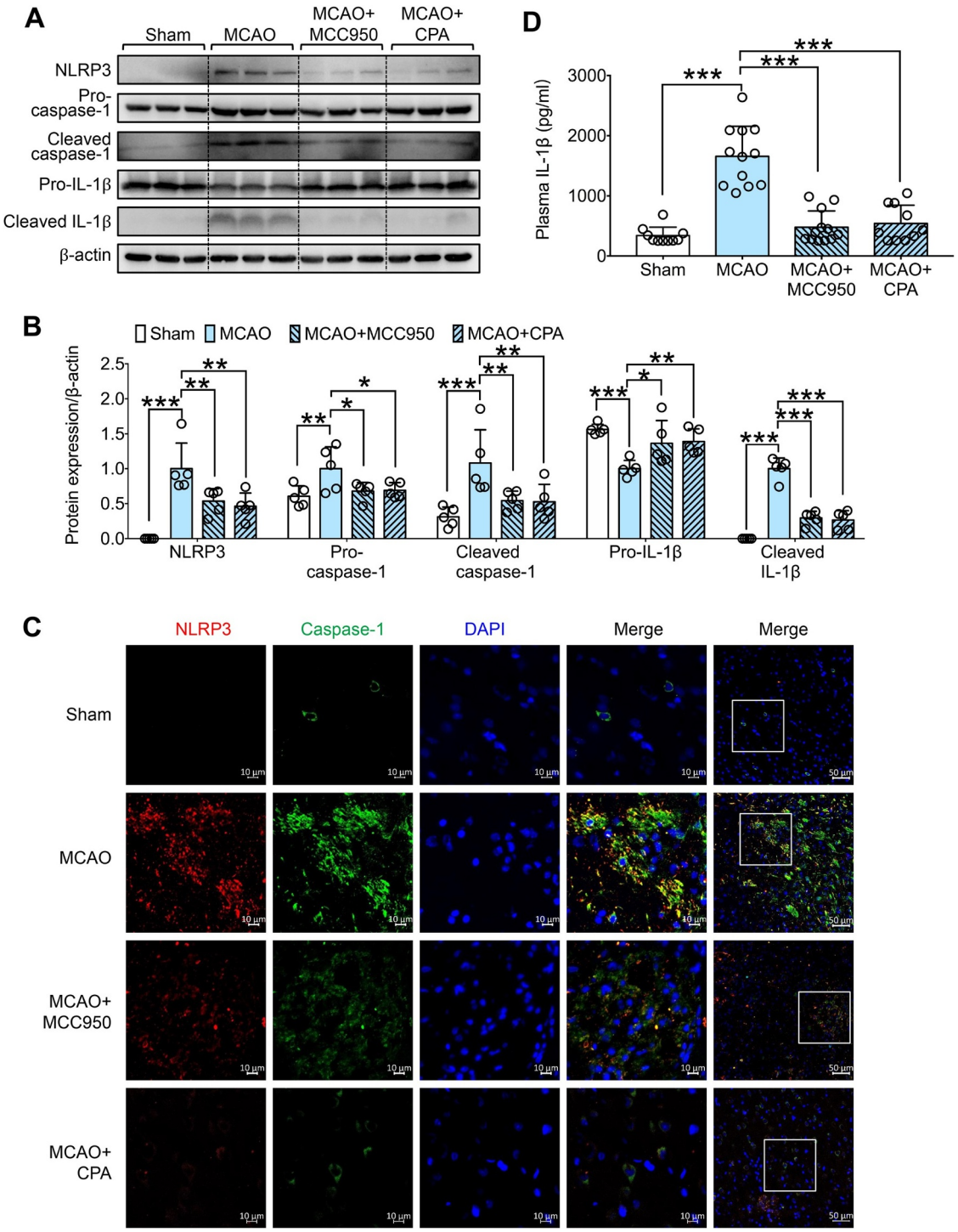

Fig. 3. CPA treatment attenuated MCAO-induced NLRP3 inflammasome activation. (**A-B**) Representative blots and quantitative analysis showing the expression of NLRP3, the cleavage of caspase-1 and IL-1β in brain tissues. (**C**) Representative confocal microscopic images showing the colocalization of NLRP3 (red) with caspase-1 (green). (**D**) Plasma level of IL-1β. * $p < 0.05$, ** $p < 0.01$, *** $p < 0.001$.

BV-2 cells (Fig. 6E-F). Consistent with our *in vivo* results, treatment with Rd and LIG alone or in combination obviously inhibited OGD/R-induced NLRP3 inflammasomes activation and consequently pyroptosis in BV-2 cells (Fig. 6A-F).

Ginsenoside Rd and Z-Ligustilide attenuated OGD/R-induced Drp1 expression and mitochondrial fission in BV-2 cells

We monitored mitochondrial morphological change using confocal microscopy in BV-2 cells. Compared with intact tubular and elongated mitochondria in control cells, punctate and shorter mitochondria were observed in OGD/R cells (Fig. 7A), indicating that OGD/R induced mitochondrial fission in BV-2 cells. It was reported that the activity of Drp1 mainly control the mitochondrial fission. To confirm Drp1-mediated mitochondrial fission in BV-2 cells, Drp1 expression was further analyzed. As expected, OGD/R increased Drp1 expression (Fig. 7B-C). Importantly, OGD/R-induced Drp1 expression and mitochondrial fission were reversed by treatment with Rd and LIG alone

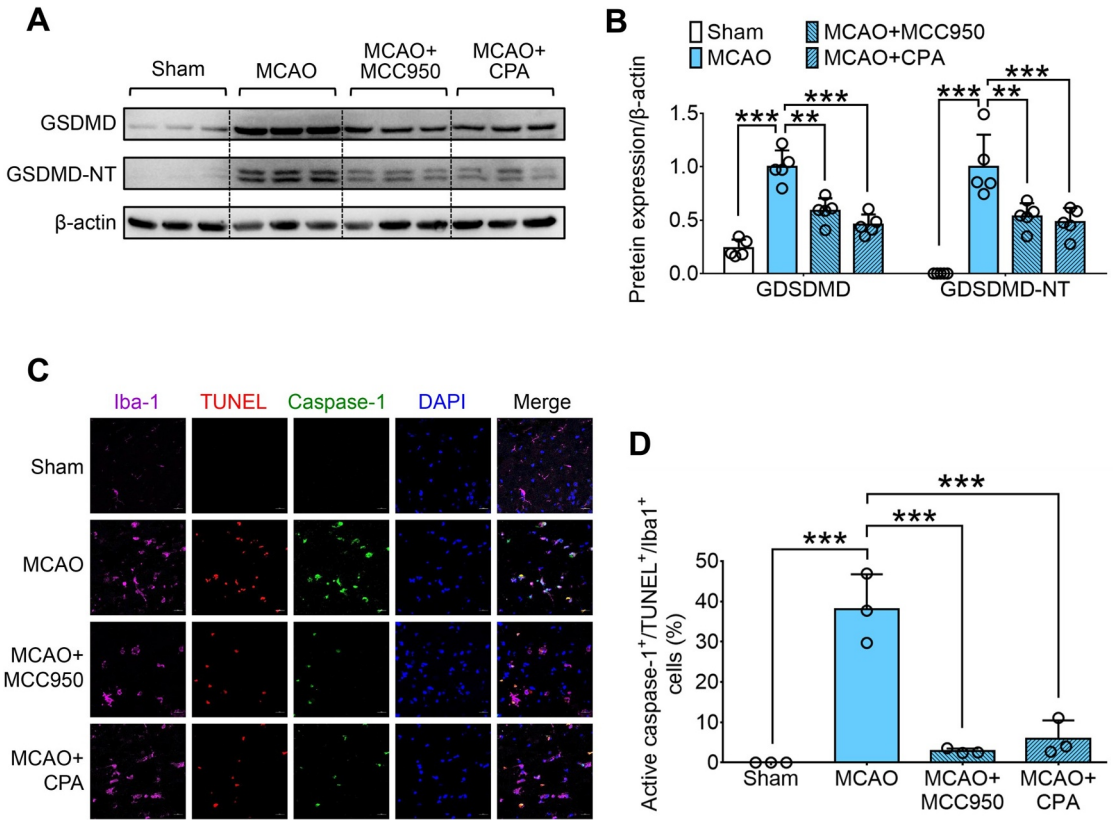

Fig. 4. CPA treatment reduced MCAO-induced microglial pyroptosis. (**A-B**) Representative blots and quantitative analysis showing the expression and cleavage of GSDMD in brain tissues. (**C-D**) Representative confocal microscopic images showing the colocalization of TUNEL (red) with active caspase-1 (green) and Iba-1 (purple) and the percentage of active caspase-1$^+$/TUNEL$^+$/Iba-1$^+$ cells (pyroptotic microglia). ** $p < 0.01$, *** $p < 0.001$.

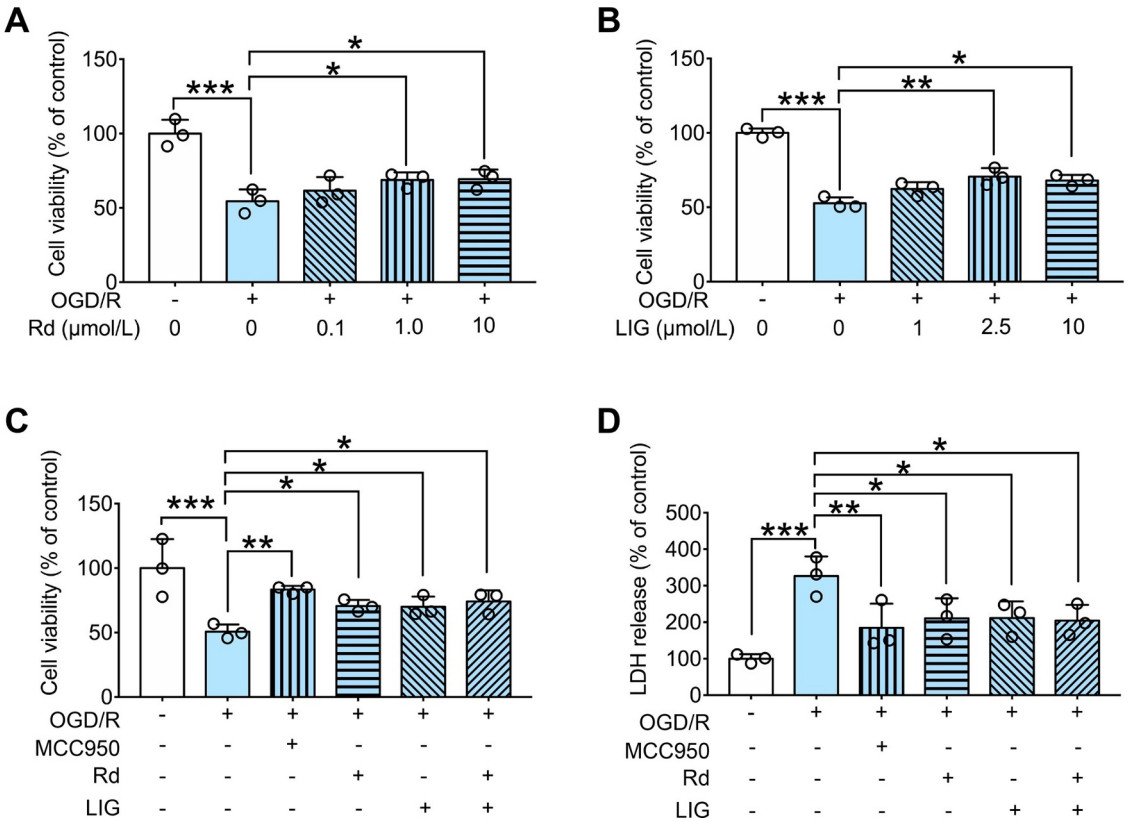

Fig. 5. Rd and LIG attenuated OGD/R-induced cell injury in BV-2 cells. (**A-B**) Cell viability in BV-2 cells treated with different concentrations of Rd and LIG (**C**) Cell viability and (**D**) LDH release in BV-2 cells. ** $p < 0.01$, *** $p < 0.001$, **** $p < 0.0001$

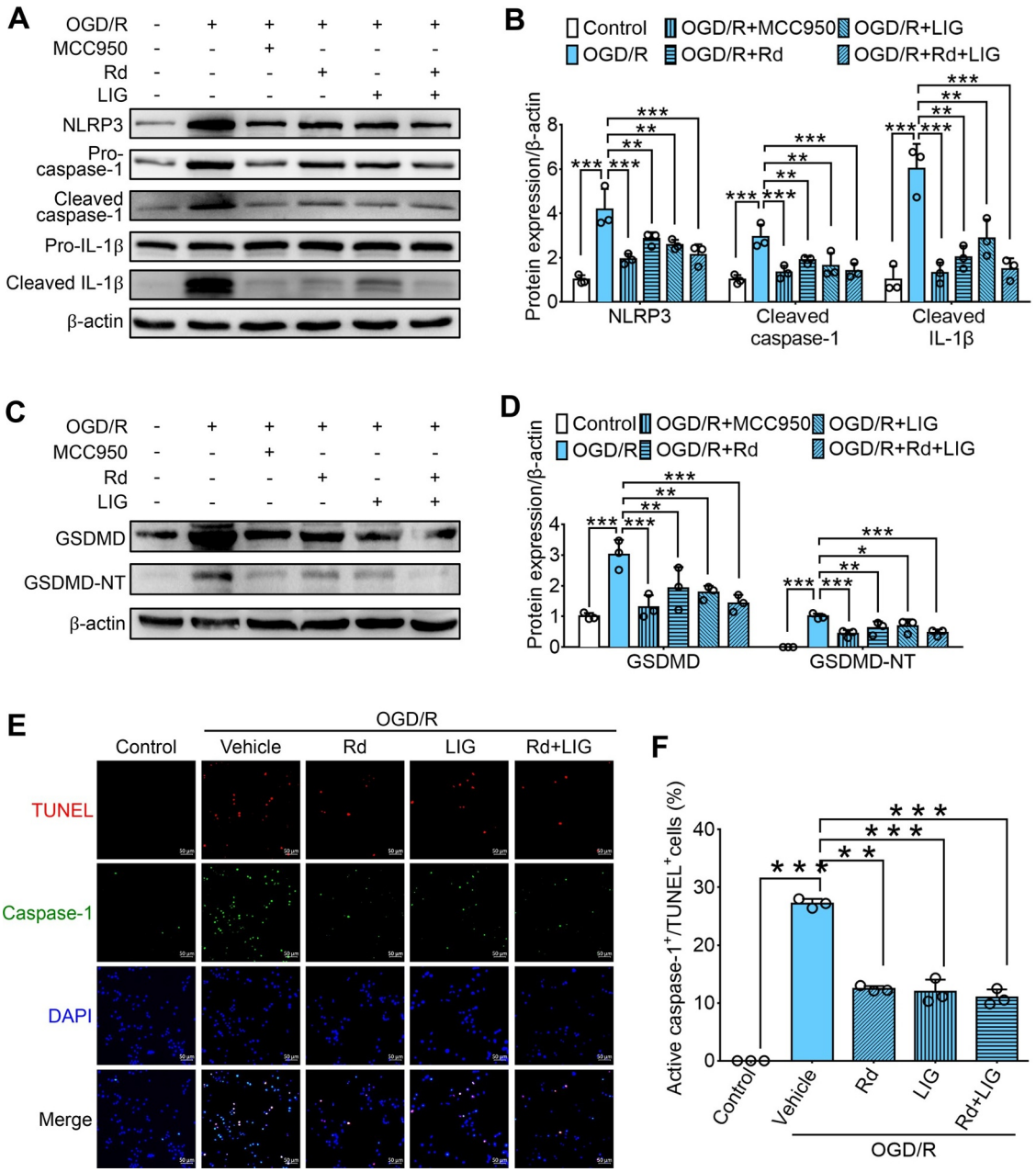

Fig. 6. Rd and LIG suppressed OGD/R-induced NLRP3 inflammasomes activation and pyroptosis in BV-2 cells. (**A-D**) Representative blots and quantitative analysis showing the expression of NLRP3, the cleavage of caspase-1, IL-1β and GSDMD. (**E-F**) Representative confocal microscopic images showing the colocalization of TUNEL (red) with active caspase-1 (green) and the percentage of active caspase-1$^+$/TUNEL$^+$ cells (pyroptotic cells). * $p < 0.05$, ** $p < 0.01$, *** $p < 0.001$.

or in combination in BV-2 cells (Fig. 7A-C). The increased expression of Drp1 was validated in MCAO rats, which was also abolished by MCC950 or CPA treatment (Fig. 7D-E).

Ginsenoside Rd and Z-Ligustilide suppressed OGD/R-induced NLRP3 inflammasome activation by inhibiting Drp1-mediated mitochondrial fission in BV-2 cells

Successful overexpression of Drp1 by the pcDNA-encoding Drp1 protein plasmid was identified by western blotting analysis (Fig. 8A-B). We found that overexpression of Drp1 significantly increased the expression of NLRP3 and promoted the subsequent cleavage of caspase-1 in BV-2 cells (Fig. 8A, C-D). Interestingly, OGD/R-induced expressions of Drp1, NLRP3 and subsequent cleavage of caspase-1 were inhibited by treatment with Rd and LIG alone and in combination, and these inhibitory effects were all abolished by overexpression of Drp1 (Fig. 8A-D). These data indicated that Rd and LIG inhibited NLRP3 inflammasomes activation by suppressing Drp1-mediated mitochondrial fission.

Ginsenoside Rd and Z-Ligustilide inhibited OGD/R-induced pyroptosis by inhibiting Drp1 expression in BV-2 cells

Contrary to control cells, in which include almost no GSDMD cleavage and no population of pyroptotic cells, OGD/R induced obviously cleavage of GSDMD (Fig. 8A, E-F) and large population of pyroptotic cells (Fig. 9A-B), and treatment with Rd and LIG alone or in combination efficiently interrupted all these events (Fig. 8A, E-F, Fig. 9A-B). Further investigation also showed that Drp1 overexpression significantly promoted OGD/R-induced pyroptosis and abolished the inhibitory effect of Rd and LIG on pyroptotic cell death (Fig. 8A, E-F, Fig. 9A-B). These results indicated that Rd and LIG inhibited OGD/R-induced pyroptosis by suppressing Drp1 expression.

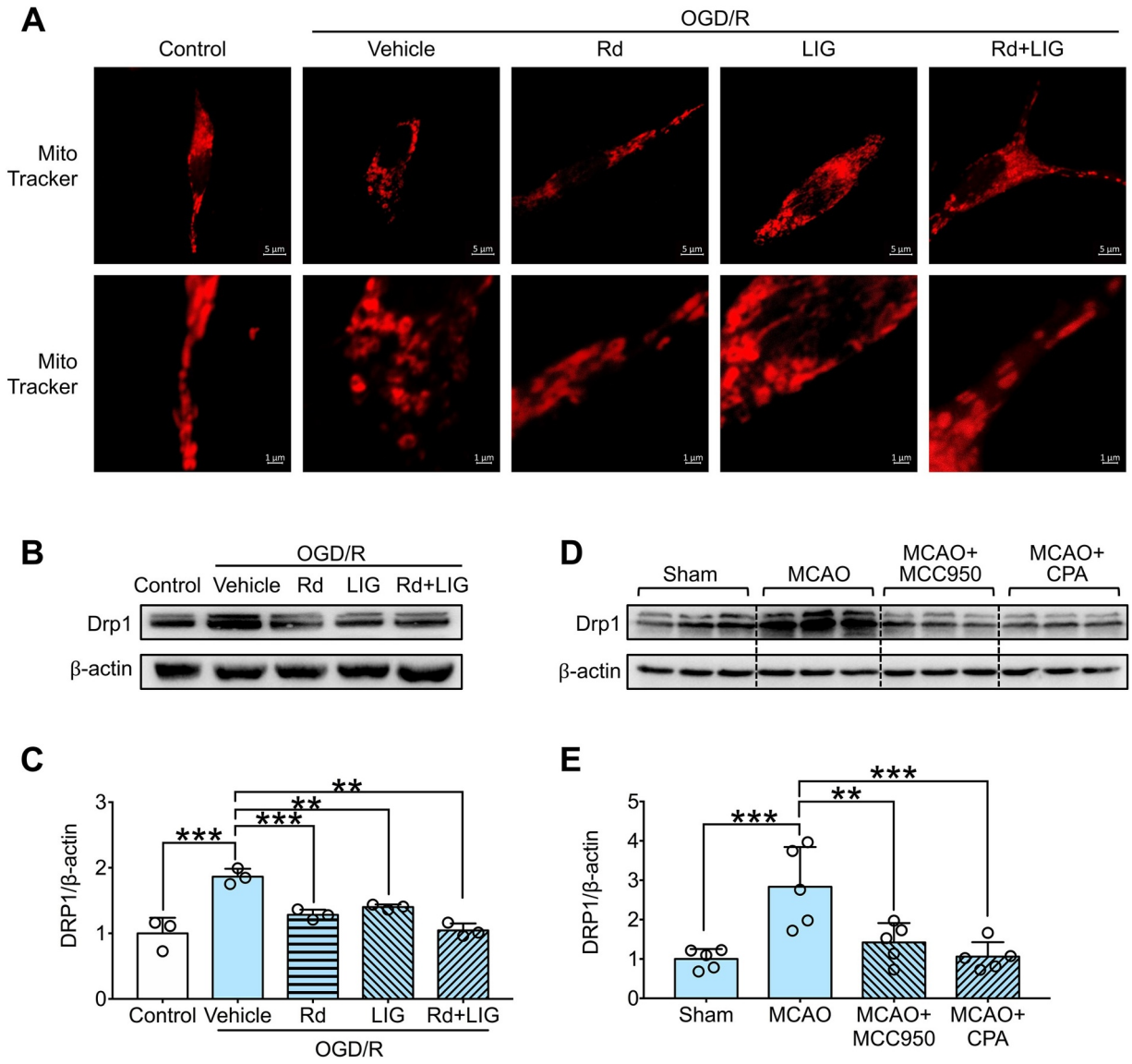

Fig. 7. Rd and LIG prevented OGD/R-induced Drp1 expression and mitochondrial fission in BV-2 cells. (**A**) Representative Mito-tracker images showing mitochondrial morphology. (**B-E**) Representative blots and quantitative analysis showing the expression of Drp1 in BV-2 cells (**B-C**) and in brain tissue of rats (**D-E**). ** $p < 0.01$, *** $p < 0.001$.

Discussion

In the current study, we demonstrated that CPA treatment ameliorated MCAO-induced cerebral damage and neurological dysfunction by inhibiting NLRP3 inflammasome activation and microglial pyroptosis. Further *in vitro* study revealed that the key active ingredients of *Panax ginseng* and *Angelica sinensis* inhibited OGD/R-induced NLRP3 inflammasome activation and pyroptosis by inhibiting Drp1-mediated mitochondrial fission.

Consistent with previous study (Xia et al., 2019), rats after MCAO exhibited significant neurological deficits, as well as obvious cerebral infarction and decreased cerebral glucose utilization in the ischemic area. Treatment with CPA considerably alleviated ischemic brain injury and showed neuroprotective effects after ischemic stroke. A Chinese herbal formula Shengui Sansheng San (SSS), which was composed of *Panax ginseng, Angelica sinensis* and *Cinnamomum cassia,* was used for ischemic stroke since early Qing dynasty (Luo et al., 2019). However, there is a lack of robust evidence to elucidate the therapeutic effect and underlying mechanism of SSS in stroke. In our study, we uncovered that CPA containing two major herbal medicines of SSS exerted significant pharmacological effect on improvement of neurological function by suppressing NLRP3 inflammasome activation and microglial pyroptosis in experimental stroke.

It was reported that stroke incidence rate and stroke prevalence in male were 33% and 41% higher than these in female respectively (Appelros et al., 2009). Toung et al pointed out the therapeutic effect of estrogen on experimental stroke in male rats (Toung et al., 1998). Considering the effect of estrogen and physiological cycle on MCAO in female rats, we chose only male rats in our study. However, the protective effect of CPA on ischemic stroke in female rats remains unknown.

NLRP3 inflammasomes activation is reported to play an important role in the pathogenesis of neurodegenerative disease and stroke (Danton and Dietrich, 2003). Lambertsen KL *et al* reported that pro-inflammatory cytokines such as IL-1 played an important role in experimental and human stroke (Lambertsen et al., 2012). Mice undergoing thromboembolic stroke exhibited enhancement of inflammasome and subsequent activation of caspase-1 and IL-1β (Abulafia et al., 2009). NLRP3 deficiency or inhibitor attenuated neurovascular damage in experimental ischemic stroke model (Ismael et al., 2018; Yang et al.,

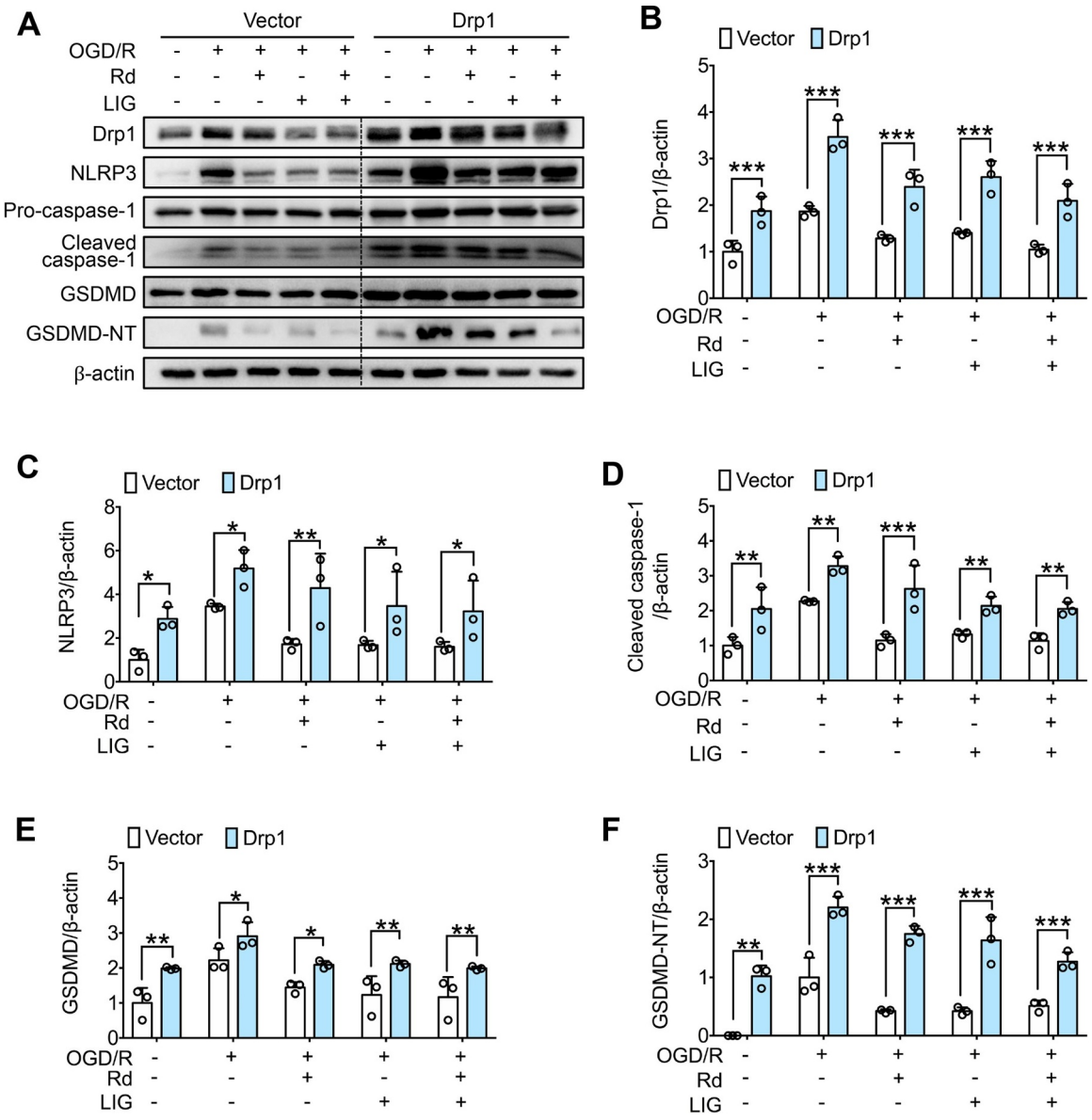

Fig. 8. Rd and LIG inhibited OGD/R-induced NLRP3 inflammasome activation and pyroptosis by down-regulating Drp1-mediated mitochondrial fission in BV-2 cells. Representative blots (**A**) and quantitative analysis showing the expression of Drp1 (**B**), NLRP3 (**C**) and GSDMD (**E**) and the cleavage of caspase-1 and GSDMD (**D, F**) in BV-2 cells. * $p < 0.05$, ** $p < 0.01$, *** $p < 0.001$.

2014). Consistent with previous studies, we found that NLRP3 inflammasome was markedly activated in cerebral infarction area and the plasma level of IL-1β significantly increased in MCAO rats. Emerging evidence showed that the major active constituents of *Panax ginseng* such as ginsenoside Rd, Rg, Rb and compound K, inhibited NLRP3 inflammasome activation in colitis, diabetes and adipose tissue (Chen et al., 2016; Liu et al., 2018). In line with these findings, we found that the administration of CPA significantly inhibited MCAO-induced NLRP3 inflammasome activation, as evidenced by decreased expression of NLRP3, cleavage of caspase-1 and IL-1β and colocalization of NLRP3 inflammasome components. Its inhibitory effect was comparable to that of MCC950, a well-known inhibitor of NLRP3 inflammasome. These results indicated that the protective effect of CPA on MCAO rats is associated with the inhibition of NLRP3 inflammasomes. Inhibiting both "priming" and "assembly" signals is related to the protective effect of CPA on ischemic stroke.

The assembly of NLRP3 inflammasome triggers the autocleavage of pro-caspase-1 into active caspase-1. In addition, caspase-1 cleaves GSDMD to yield GSDMD-NT, which critically determines the fate of pyroptotic cell death (Shi et al., 2017). Driven by inflammasome activation, pyroptotic cell death in microglia exacerbated brain damage in stroke (Fann et al., 2013; Poh et al., 2019). Consistent with previous reports, we found that MCAO promoted the cleavage of GSDMD in ischemic brain tissue, indicating the presence of pyroptosis in the ischemic area.

Pyroptotic cells share some common features with apoptotic cells, including DNA fragmentation which can be labeled by TUNEL-staining (Labbe and Saleh, 2008). It was reported that the activation of microglia, the major resident immune cells in the brain, triggered deleterious inflammatory reaction in transient global ischemia (Hanisch and Kettenmann, 2007). To identify the cell type of pyroptosis, triple-immunostaining of active caspase-1, TUNEL and the microglial marker Iba-1 was performed in our study. Interestingly, the majority of pyroptotic cells were activated microglia. Two ginsenosides, which are found in Korean Red Ginseng, strongly inhibited inflammasome-mediated pyroptosis triggered by Listeria monocytogenes in macrophages (Kim et al., 2014). We further disclosed that the administration of CPA and MCC950 inhibited the cleavage of GSDMD and reduced the number

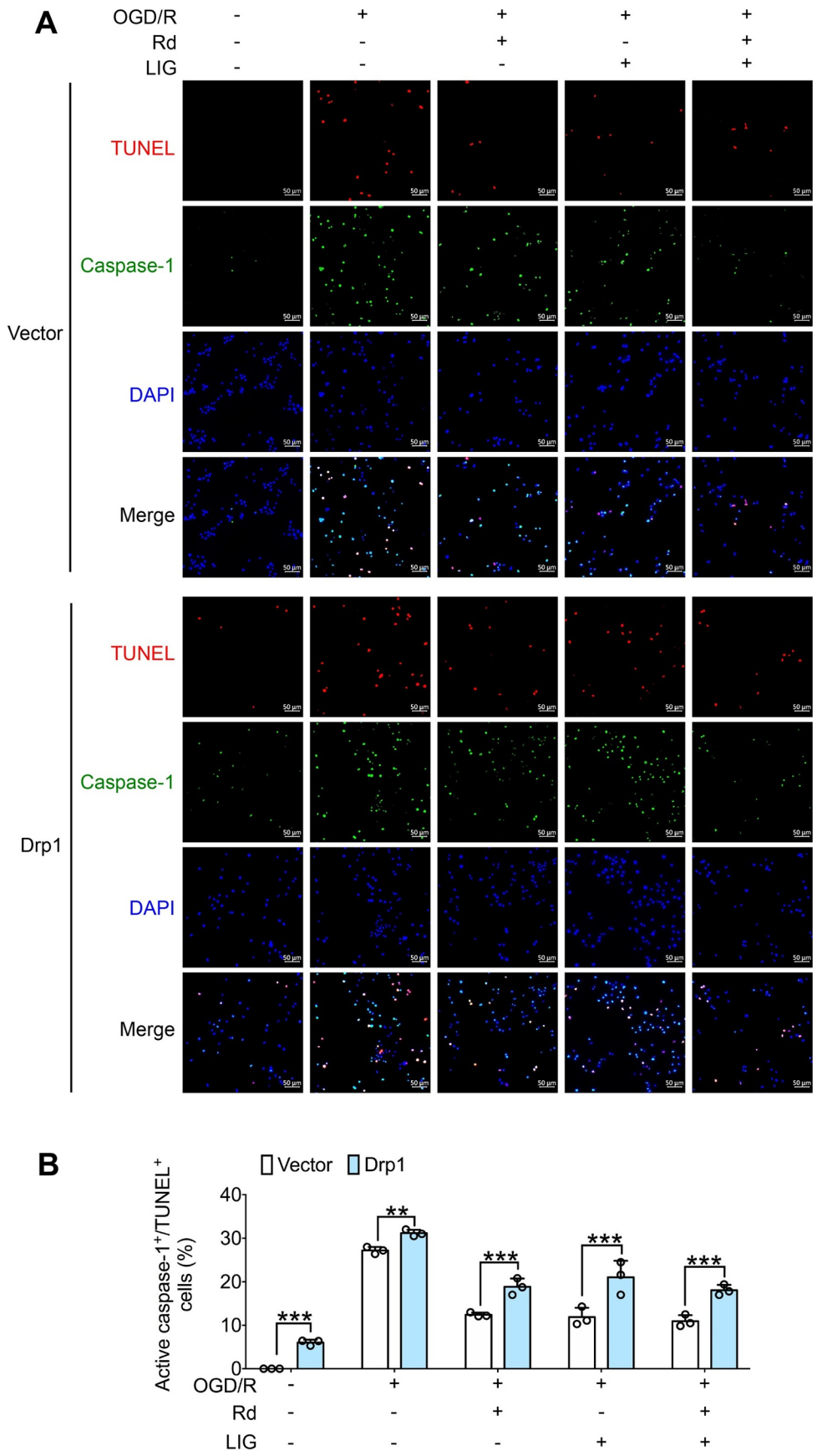

Fig. 9. Rd and LIG reduced OGD/R-induced pyroptosis by inhibiting Drp1 expression in BV-2 cells. (**A**) Representative confocal microscopic images showing the colocalization of TUNEL (red) with active caspase-1 (green) and (**B**) the percentage of active caspase-1$^+$/TUNEL$^+$ cells (pyroptotic cells). * $p < 0.05$, *** $p < 0.001$.

of pyroptotic microglia. It is reasonable that CPA's neuroprotective effect is related to inhibiting NLRP3 inflammasomes activation and microglial pyroptosis in experimental stroke rats.

Considering the majority of pyroptotic cells were activated microglia in MCAO rats, BV-2 cells line subjected to OGD/R were used to detect whether CPA treatment inhibited NLRP3 inflammasomes and related pyroptosis *in vitro*. Accumulating evidence supported that NLRP3 inflammasome pathway was activated under OGD/R condition (Fann et al., 2013). Correspondingly, we confirmed that OGD/R activated NLRP3 inflammasome and induced pyroptosis in BV-2 cells, as evidenced by increased LDH release, the cleavage of GSDMD and the existence of active caspase-1^+/TUNEL$^+$ cells. OGD/R-induced activation of NLRP3 inflammasomes and related pyroptosis were inhibited by treatment with Rd and LIG alone or in combination.

Mitochondrial fission is an early event involved in the brain injury of ischemic stroke, which is mediated by Drp1, a cytosolic protein that can translocate to the outer mitochondrial membrane on activation (Korobova et al., 2013). The imbalance of mitochondrial dynamics controls the mitochondrial morphology and function. Accumulation of damaged mitochondria triggered NLRP3 inflammasome activation by releasing mitochondrial reactive oxygen species or mitochondrial DNA into the cytosol (Park et al., 2013). Souvarish Sarkar *et al* reported that impaired mitochondrial function augmented the NLRP3 inflammasome-driven proinflammatory cascade in microglia (Sarkar et al., 2017). Here we clearly presented that Drp1 acted as an upstream factor regulated by OGD/R injury, and thus leading to the NLRP3 inflammasome activation and pyroptosis in microglia, which were reversed by treatment with Rd and LIG. Moreover, increased expression of Drp1 and mitochondrial fission were validated in MCAO rats, which were also abolished by MCC950 or CPA treatment. We further overexpressed Drp1 to confirm whether Rd and LIG inhibited NLRP3 inflammasome activation by inhibiting Drp1-mediated mitochondrial fission. Our results demonstrated for the first time that overexpression of Drp1 abrogated the protective effects of Rd and LIG on inhibiting OGD/R-induced NLRP3 inflammasome activation and related pyroptosis. Taken together, Rd and LIG solely or in combination directly inhibited OGD/R-induced Drp1-mediated mitochondrial fission, thus leading to inactivation of NLRP3 inflammasome and inhibition of pyroptosis.

Collectively, the results we presented here reveal that CPA exerts neuroprotective effects by inhibiting NLRP3 inflammasome activation and related pyroptosis. Moreover, we uncovered its protective effect at least partially through inhibiting Drp1-mediated mitochondrial fission. Our study identifies the benefit of CPA for ischemic stroke and provides more evidences for therapeutical value of CPA on diseases which are associated with NLRP3 inflammasome and related pyroptosis.

Funding

This work was supported by the Natural Science Foundation of Guangdong province (grant number 2017A030311017), the National Natural Science Foundation of China (grant numbers 81873514, 81570394 and 81370371) and Guangxi Natural Science Foundation (2018GXNSFAA294102).

Credit author statement

Hongmei Tan designed the research and got the funding. Jia Hu performed the experiment and data analysis, and drafted the manuscript. Cheng Zeng carried out the experiment, data collection and interpretation. Jie Wei, Fengqi Duan and Sijun Liu were responsible for methodology and software. Yonghua Zhao and Hongmei Tan revised the manuscript. All authors read and approved the final manuscript.

Declaration of Competing Interest

None.

Supplementary materials

Supplementary material associated with this article can be found, in the online version, at doi:10.1016/j.phymed.2020.153251.

References

Abulafia, D.P., de Rivero Vaccari, J.P., Lozano, J.D., Lotocki, G., Keane, R.W., Dietrich, W.D., 2009. Inhibition of the inflammasome complex reduces the inflammatory response after thromboembolic stroke in mice. J Cereb Blood Flow Metab 29, 534–544.
Appelros, P., Stegmayr, B., Terent, A., 2009. Sex differences in stroke epidemiology: a systematic review. Stroke 40, 1082–1090.
Barrington, J., Lemarchand, E., Allan, S.M., 2017. A brain in flame; do inflammasomes and pyroptosis influence stroke pathology? Brain Pathol 27, 205–212.
Chen, W., Wang, J., Luo, Y., Wang, T., Li, X., Li, A., Li, J., Liu, K., Liu, B., 2016. Ginsenoside Rb1 and compound K improve insulin signaling and inhibit ER stress-associated NLRP3 inflammasome activation in adipose tissue. J Ginseng Res 40, 351–358.
Danton, G.H., Dietrich, W.D., 2003. Inflammatory mechanisms after ischemia and stroke. J Neuropathol Exp Neurol 62, 127–136.
Davis, B.K., Wen, H., Ting, J.P., 2011. The inflammasome NLRs in immunity, inflammation, and associated diseases. Annu Rev Immunol 29, 707–735.
Fann, D.Y., Lee, S.Y., Manzanero, S., Tang, S.C., Gelderblom, M., Chunduri, P., Bernreuther, C., Glatzel, M., Cheng, Y.L., Thundyil, J., Widiapradja, A., Lok, K.Z., Foo, S.L., Wang, Y.C., Li, Y.I., Drummond, G.R., Basta, M., Magnus, T., Jo, D.G., Mattson, M.P., Sobey, C.G., Arumugam, T.V., 2013. Intravenous immunoglobulin suppresses NLRP1 and NLRP3 inflammasome-mediated neuronal death in ischemic stroke. Cell Death Dis 4, e790.
Hanisch, U.K., Kettenmann, H., 2007. Microglia: active sensor and versatile effector cells in the normal and pathologic brain. Nat Neurosci 10, 1387–1394.
Hu, G., Wu, Z., Yang, F., Zhao, H., Liu, X., Deng, Y., Shi, M., Zhao, G., 2013. Ginsenoside Rd blocks AIF mitochondrio-nuclear translocation and NF-kappaB nuclear accumulation by inhibiting poly(ADP-ribose) polymerase-1 after focal cerebral ischemia in rats. Neurol Sci 34, 2101–2106.
Ismael, S., Zhao, L., Nasoohi, S., Ishrat, T., 2018. Inhibition of the NLRP3-inflammasome as a potential approach for neuroprotection after stroke. Sci Rep 8, 5971.
Kim, J., Ahn, H., Han, B.C., Lee, S.H., Cho, Y.W., Kim, C.H., Hong, E.J., An, B.S., Jeung, E.B., Lee, G.S., 2014. Korean red ginseng extracts inhibit NLRP3 and AIM2 inflammasome activation. Immunol Lett 158, 143–150.
Korobova, F., Ramabhadran, V., Higgs, H.N., 2013. An actin-dependent step in mitochondrial fission mediated by the ER-associated formin INF2. Science 339, 464–467.
Kuang, X., Yao, Y., Du, J.R., Liu, Y.X., Wang, C.Y., Qian, Z.M., 2006. Neuroprotective role of Z-ligustilide against forebrain ischemic injury in ICR mice. Brain Res 1102, 145–153.
Labbe, K., Saleh, M., 2008. Cell death in the host response to infection. Cell Death Differ 15, 1339–1349.
Lambertsen, K.L., Biber, K., Finsen, B., 2012. Inflammatory cytokines in experimental and human stroke. J Cereb Blood Flow Metab 32, 1677–1698.
Li, J., Hua, Y., Ji, P., Yao, W., Zhao, H., Zhong, L., Wei, Y., 2016. Effects of volatile oils of Angelica sinensis on an acute inflammation rat model. Pharm Biol 54, 1881–1890.
Liu, C., Wang, J., Yang, Y., Liu, X., Zhu, Y., Zou, J., Peng, S., Le, T.H., Chen, Y., Zhao, S., He, B., Mi, Q., Zhang, X., Du, Q., 2018. Ginsenoside Rd ameliorates colitis by inducing p62-driven mitophagy-mediated NLRP3 inflammasome inactivation in mice. Biochem Pharmacol 155, 366–379.
Luo, C., Bian, X., Zhang, Q., Xia, Z., Liu, B., Chen, Q., Ke, C., Wu, J.L., Zhao, Y., 2019. Shengui Sansheng San Ameliorates Cerebral Energy Deficiency via Citrate Cycle After Ischemic Stroke. Front Pharmacol 10, 386.
Park, S., Juliana, C., Hong, S., Datta, P., Hwang, I., Fernandes-Alnemri, T., Yu, J.W., Alnemri, E.S., 2013. The mitochondrial antiviral protein MAVS associates with NLRP3 and regulates its inflammasome activity. J Immunol 191, 4358–4366.
Poh, L., Kang, S.W., Baik, S.H., Ng, G.Y.Q., She, D.T., Balaganapathy, P., Dheen, S.T., Magnus, T., Gelderblom, M., Sobey, C.G., Koo, E.H., Fann, D.Y., Arumugam, T.V., 2019. Evidence that NLRC4 inflammasome mediates apoptotic and pyroptotic microglial death following ischemic stroke. Brain Behav Immun 75, 34–47.
Sarkar, S., Malovic, E., Harishchandra, D.S., Ghaisas, S., Panicker, N., Charli, A., Palanisamy, B.N., Rokad, D., Jin, H., Anantharam, V., Kanthasamy, A., Kanthasamy, A.G., 2017. Mitochondrial impairment in microglia amplifies NLRP3 inflammasome proinflammatory signaling in cell culture and animal models of Parkinson's disease. NPJ Parkinsons Dis 3, 30.
Schroder, K., Tschopp, J., 2010. The inflammasomes. Cell 140, 821–832.
Shi, J., Gao, W., Shao, F., 2017. Pyroptosis: Gasdermin-Mediated Programmed Necrotic Cell Death. Trends Biochem Sci 42, 245–254.

Toung, T.J., Traystman, R.J., Hurn, P.D., 1998. Estrogen-mediated neuroprotection after experimental stroke in male rats. Stroke 29, 1666–1670.
Wang, J., Chao, F., Han, F., Zhang, G., Xi, Q., Li, J., Jiang, H., Wang, J., Yu, G., Tian, M., Zhang, H., 2013. PET demonstrates functional recovery after transplantation of induced pluripotent stem cells in a rat model of cerebral ischemic injury. J Nucl Med 54, 785–792.
Xia, Z.Y., Luo, C., Liu, B.W., Bian, X.Q., Li, Y., Pang, A.M., Xu, Y.H., Tan, H.M., Zhao, Y.H., 2019. Shengui Sansheng Pulvis maintains blood-brain barrier integrity by vasoactive intestinal peptide after ischemic stroke. Phytomedicine 67, 153158.
Yang, F., Wang, Z., Wei, X., Han, H., Meng, X., Zhang, Y., Shi, W., Li, F., Xin, T., Pang, Q., Yi, F., 2014. NLRP3 deficiency ameliorates neurovascular damage in experimental ischemic stroke. J Cereb Blood Flow Metab 34, 660–667.
Ye, R., Yang, Q., Kong, X., Han, J., Zhang, X., Zhang, Y., Li, P., Liu, J., Shi, M., Xiong, L., Zhao, G., 2011. Ginsenoside Rd attenuates early oxidative damage and sequential inflammatory response after transient focal ischemia in rats. Neurochem Int 58, 391–398.
Zeng, C., Wang, R., Tan, H., 2019. Role of Pyroptosis in Cardiovascular Diseases and its Therapeutic Implications. Int J Biol Sci 15, 1345–1357.